

# Web of Science Search

## JOURNAL SEARCH

### SUBMITTING A JOURNAL?

Build bibliographies in more than 5,000 different styles.

with **EndNote**

[endnote.com](http://endnote.com) >

Search Terms: GEOCHEMISTRY

Total journals found: 9

THE FOLLOWING TITLE(S) MATCHED YOUR REQUEST:

Journals 1-9 (of 9)

FORMAT FOR PRINT

#### APPLIED GEOCHEMISTRY

Monthly ISSN: 0883-2927

PERGAMON-ELSEVIER SCIENCE LTD, THE BOULEVARD, LANGFORD LANE, KIDLINGTON, OXFORD, ENGLAND, OX5 1GB

Coverage

#### AQUATIC GEOCHEMISTRY

Quarterly ISSN: 1380-6185

SPRINGER, 233 SPRING ST, NEW YORK, USA, NY, 10013

Coverage

#### CHEMIE DER ERDE-GEOCHEMISTRY

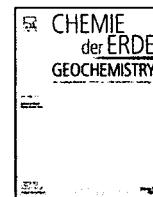
Quarterly ISSN: 0009-2819

ELSEVIER GMBH, URBAN & FISCHER VERLAG, OFFICE JENA, P O BOX 100537, JENA, GERMANY, 07705

Coverage

Science Citation Index Expanded

Current Contents - Physical, Chemical & Earth Sciences



## Mixing geochemistry of cold water around non-volcanic thermal springs in high-grade metamorphic terrain, Sri Lanka

D.T. Jayawardana<sup>a,\*</sup>, D.T. Udagedara<sup>b</sup>, A.A.M.P. Silva<sup>b</sup>, H.M.T.G.A. Pitawala<sup>c</sup>,  
W.K.P. Jayathilaka<sup>b</sup>, A.M.N.M. Adikaram<sup>d</sup>

<sup>a</sup> Sri Jayawardanepura University, Faculty of Applied Science, Department of Forestry and Environmental Science, Gangodawila, Nugegoda, Sri Lanka

<sup>b</sup> Uva Wellassa University, 90000 Badulla, Sri Lanka

<sup>c</sup> Department of Geology, Faculty of Science, University of Peradeniya, Sri Lanka

<sup>d</sup> Department of Physical Sciences, Faculty of Applied Sciences, South Eastern University, Sri Lanka

### ARTICLE INFO

#### Article history:

Received 5 February 2016

Received in revised form 18 October 2016

Accepted 19 October 2016

#### Keywords:

Thermal water  
Cold water  
Geochemistry  
Geothermometer  
Mixing

### ABSTRACT

A geochemical survey was conducted on thermal water and cold water around non-volcanic geothermal fields at Mahaoya and Marangala in Sri Lanka. One hundred forty-two samples were analyzed for fifteen selected ions to investigate geochemical relationships resulting from water–rock interactions and mixing. Based on measurements using a Na–K–Mg geothermometer, the maximum temperatures of thermal reservoirs were estimated to be 148 °C in Mahaoya and 191 °C in Marangala, which were higher values than those obtained using Na–Li and Li–Mg geothermometers. This suggests that the reservoirs extend from intermediate to deep levels. Hydrogeochemistry of thermal waters is distinct from that of cold water; higher contents of Na, K, Cl, F, SO<sub>4</sub> and TDS in thermal water are most likely due to the dissolution of feldspar, mica, and sulfide minerals in the granitic rocks. Conversely, lower values of Fe, Mg, Cu, Zn, and Pb imply less ferromagnesian minerals in the basement. Classification based on major ions reveals a Na–K–SO<sub>4</sub> type of thermal water for Mahaoya and Marangala. Cold water is dominated by the Na–K–HCO<sub>3</sub> type, which indicates deep groundwater influence by iron exchange. Non-mixing cold water indicates a Ca–HCO<sub>3</sub> type. In general, chemistry of cold water wells (<400 m) close to the thermal water changes significantly due to direct mixing of thermal water and cold water. In comparison, a contrasting action occurs with increasing distance from the geothermal field. Gradual decline of SO<sub>4</sub> with increasing distance from thermal water may indicate a trend of clear oxidation. However, the chemistry of more distant wells demarcates deep circulations through fractures and faults in the basement.

© 2016 Elsevier GmbH. All rights reserved.

### 1. Introduction

Thermal springs are volcanic or non-volcanic in origin. Volcanic thermal springs are mainly found in areas with volcanic activity (Mutlu and Gulec, 1998; Gemici and Tarcan, 2002; Du et al., 2005; Sanada et al., 2006; Papp and Nitoi, 2006; Pasvanoğlu and Chandrasekharam, 2011; Navarro et al., 2011; Taran et al., 2013; Petrini et al., 2013). Non-volcanic thermal springs are located in metamorphic and igneous terrains such as Sri Lanka, India, Malaysia, Japan, Canada, and Indonesia (Chandrasekharam and

Antu, 1995; Jessop et al., 1991; Dissanayake and Jayasena, 1988). Studies on non-volcanic thermal springs have received less attention worldwide than studies on volcanic thermal springs (Brugger et al., 2005; Yaguchi et al., 2014; Baioumy et al., 2015).

Both volcanic and non-volcanic thermal springs impact hydro geochemistry in their respective area (Pasvanoğlu and Chandrasekharam, 2011; Gibson and Hinman, 2013). The quality of cold water surrounding thermal springs can change due to different sources of geothermal fluid (Navarro et al., 2011) and mixing of thermal water with deep cold water, infiltrated shallow groundwater, and sea water (Han et al., 2010; Petrini et al., 2013; Gibson and Hinman, 2013). Mixing modifies chemical signatures and compositions depending on the level of water–rock interaction around the geotherm (Pasvanoğlu and Chandrasekharam, 2011; Taran et al., 2013). Hydrogeochemical indicators, such as major ion ratios, can be used to study origin and mixing (Capasso et al., 2001; Gibson and

\* Corresponding author.

E-mail addresses: daham@sci.sjp.ac.lk, tarangaj@gmail.com (D.T. Jayawardana), tharangau@yahoo.com (D.T. Udagedara), aruna.manoj.prasad@gmail.com (A.A.M.P. Silva), apitawala@pdn.ac.lk (H.M.T.G.A. Pitawala), priyanthikajayathilaka@yahoo.com (W.K.P. Jayathilaka), maduryaa@gmail.com (A.M.N.M. Adikaram).

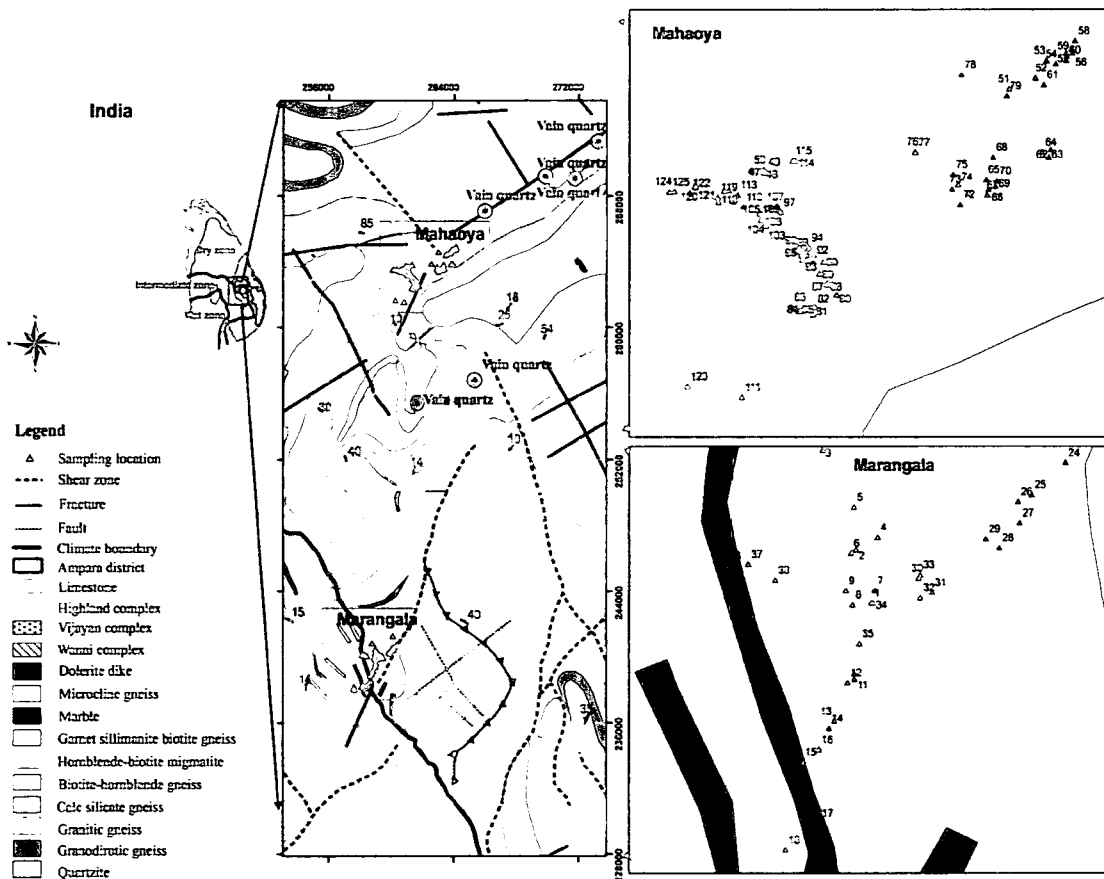


Fig. 1. Geology and structural geology of Mahaoya and Marangala area that shows the hot springs and sampling locations.

Hinman, 2013). Physico-chemical data in aquifers may also indicate structural elements of geothermal systems (Favara et al., 2001).

A non-volcanic thermal spring line in Sri Lanka is found on the boundary between two major lithological groups in high-grade metamorphic rocks of Precambrian age (Fig. 1). The estimated temperatures of this line are a potential source of geothermal energy (Dissanayake and Jayasena, 1988; Mangala and Wijetilake, 2011). Studies along the line have demarcated the dolerite dike for thermal water circulations (Senaratne and Chandima, 2011), whereas the dolerite dike is not the source of heat (Nimalsiri et al., 2015). The deep percolated water-absorbing heat may originate from hot dry rock (Kumara and Dharmagunawardhane, 2014). Chandrajith et al. (2013) has stated that heterogeneous geothermal gradients heat the thermal spring line. However, the origin and structure of the thermal water are still unknown. Furthermore, little research has been published on the study of water-rock interaction and mixing of thermal water with surrounding cold water. To fill this gap, the objective of this study is to investigate geochemical relationships due to water-rock interaction and subsequent mixing of thermal and cold water in the non-volcanic geothermal zone of Mahaoya and Marangala in Sri Lanka.

## 2. Site description

### 2.1. Physical settings of the thermal spring

Mahaoya and Marangala springs are located in Ampara district, located 330 km from the capital city of Colombo. These springs create clusters along the thermal spring line of the country (Fig. 1; Dissanayake and Jayasena, 1988). Mahaoya has seven and Marangala has three natural springs, respectively, located 45 m

above mean sea level. The open thermal wells of Mahaoya and Marangala are distant from the sea; therefore, no direct mixing with seawater occurs. Both locations falls within the basin of the Mahaoya River that flows from south-west to north-east (Cooray, 1984). Wellhead temperatures of Mahaoya are reported to be the highest (55 °C) among the thermal spring line of the country, while Marangala reported relatively lower values (47 °C).

### 2.2. Geological setting

Over 90% of the Precambrian basement of Sri Lanka is comprised of metamorphic rocks (Fig. 1; Cooray, 1994). The basement is divided into three major lithological units known as granulite facies Highland Complex (ages 1942–650 Ma; Kröner et al., 1991) and amphibolite facies Wannai and Vijayan Complexes (ages 1100–550 Ma; Kröner et al., 1991). The sampling sites are located around the boundary between the Highland and Vijayan Complexes, which are considered to be a mineralized belt or thrust zone (Dissanayake and Munasinghe, 1984; Kröner et al., 1991).

Mahaoya and Marangala springs are located on granitic gneiss and hornblende-biotite migmatite. In addition, biotite-hornblende gneiss, garnet-sillimanite-biotite gneiss, and microcline gneiss are common in the area (Fig. 1). Dolerite dikes with marble and calc silicate gneiss can be observed, especially around the Marangala springs (Cooray, 1984, 1994; Senaratne and Chandima, 2011).

### 2.3. Hydrological setting

The groundwater flow system of Sri Lanka has been widely studied (Dissanayake and Weerasooriya, 1986; Panabokke and Perera, 2005; Villholth and Rajasooriyar, 2010). Water recharge occurs in

the central regions (>1000 ft), and a centrifugal water flow pattern brings that water to the dry zone discharge regions (Herath, 1984). The study sites contain shallow and deep regolith aquifers, which have their own recharge and discharge systems that are sensitive to northeast monsoons. The deep regolith aquifers have a continuous body of groundwater that is linked to the regional water table. The water-bearing formation of the area is weathered basement, and deep fractures exist in basement rocks (Panabokke and Perera, 2005). The water table fluctuates over a range of a few meters depending on monsoons and inter-monsoons. The water table is lower in the dry season and dramatically higher in the rainy season.

#### 2.4. Climatic condition

The eastern regions of the dry zone in Sri Lanka have mountainous terrain in the western margin (Fig. 1). This zone receives 1750 mm mean annual rainfall from northeast monsoons during October to December. The average annual temperature and evaporation of the area are 33 °C and 1400 mm, respectively. Generally, there is a long dry period from May to August (Panabokke, 1996; Chandrapala and Wimalasuriya, 2003), mainly due to the lack of rainfall during the southwest monsoons that cover the mountain range in the western margin.

### 3. Materials and methods

#### 3.1. Sample collection, preparation, and analyses

A detailed survey was performed prior to sampling. One hundred forty-two samples were collected during the intermediate season (February–March) in the sampling locations of Mahaoya ( $n=7$ ) and Marangala ( $n=3$ ) thermal springs (Fig. 1). Groundwater and surface water samples were collected randomly within a three-kilometer radius for both locations. Collected samples were stored immediately in a <4 °C cooling box for laboratory analyses.

The quantity of selected trace elements in the samples was determined by using atomic absorption spectroscopy (AAS; Varian 240 series). The flame atomic absorption version of the instrument was used according to standard procedures; the instrument was linearly calibrated with custom single-element standards (Ahmed et al., 2010). The detection limit of the instrument is 1 µg/L, and the average accuracy and precision were less than 2% error.

Selected anions were measured using a spectrophotometer and titration. The concentrations of fluoride in the samples were analyzed using a spectrophotometer (UV1600/1800 UV/VIS scanning spectrophotometer). The accuracy and precision for the analyses were 1%, and the photometric measuring range was  $\pm 3$  Abs (Zielinski et al., 2011; Ensafi and Kazemzadeh, 1999). The concentrations of chloride (Cl) were determined by titration of 25 mL samples with 0.014 M silver nitrate (AgNO<sub>3</sub>) using potassium chromate (K<sub>2</sub>CrO<sub>4</sub>) as an indicator. The bicarbonate (HCO<sub>3</sub>) concentration in the samples was measured by titration with the standard 0.01 M sulfuric acid (H<sub>2</sub>SO<sub>4</sub>). Sulfate (SO<sub>4</sub>) was measured by precipitation with standard barium chloride (BaCl<sub>2</sub>) under acidic pH. The average estimated error for the titration was  $\pm 0.5\%$ . In general, for most of the groundwater samples iron charge, imbalances were less than 5%, although it is slightly higher in the thermal spring waters.

For each sample, field tests were performed for selected physical properties. Electrical conductivity (EC), total dissolved solids (TDS), pH, and the oxidation reduction potential (ORP) of the water samples were directly measured using a portable Horiba D-73 combined instrument (Rikagaku kenkujo, Japan), which was calibrated for pH and TDS by means of a standard calibration procedure. Aver-

age accuracy for EC, TDS, pH, and ORP were  $\pm 0.5\%$ ,  $\pm 10$  ppm,  $\pm 0.1$ , and  $\pm 10$  mV, respectively, with approximately 1–5% precision.

### 4. Results and discussion

#### 4.1. Chemistry of thermal spring and cold water

Table 1 presents concentration ranges and mean values for the analyzed elements of the thermal springs. The concentrations of Na (Avg. 427 mg/L; Range 198–535 mg/L), K (Avg. 18 mg/L; Range, 14–33 mg/L) and Ca (Avg. 59 mg/L; Range 17–88 mg/L) for Mahaoya and Marangala thermal springs were higher (Table 1), whereas the average Mg concentration was lower with respect to other elements (0.85 mg/L). The average concentrations of SO<sub>4</sub> (280 mg/L), F (6.9 mg/L), and Cl (88 mg/L) were significantly higher in thermal springs. However, the HCO<sub>3</sub> concentration was relatively low (Avg. 101 mg/L).

A statistical summary of the analyzed cold waters is presented in Table 1. Concentrations of Na, K, Ca, and Mg in dug wells, tube wells, and streams were higher than surface water springs (Table 1). The average content of Al was higher in tube wells than in other cold waters. The average F, Cl, SO<sub>4</sub>, and HCO<sub>3</sub> concentrations in dug wells and tube wells were higher (Table 1), whereas streams and natural springs are characterized by lower contents. In particular, F was significantly enriched in dug wells (Avg. 3.6 mg/L) and tube wells (Avg. 8.0 mg/L).

Conversely, the average concentrations of Na, K, Ca, and SO<sub>4</sub> in thermal springs were significantly higher than those in the cold water (Table 1). The thermal springs had the lowest average Mg concentration. The average concentrations of F and Cl were higher in thermal water than dug wells, surface springs, and streams, whereas tube wells had the highest average value. The average level of HCO<sub>3</sub> in thermal springs was significantly lower than that in cold water, with the exception of surface spring water.

Generally, a significant level of charge imbalance exists in Mahaoya and Marangala thermal waters. Cations are more dominant than anions in the system, so a higher charge balance error was reported. This suggests that the high concentrated water availability in the Mahaoya and Marangala thermal systems is due to dissolution of major cations in primary minerals.

#### 4.2. Physico-chemical signature of thermal springs and cold water

Table 1 shows the summary of results for the physico-chemical parameters in thermal springs and cold waters. The collected water is characterized by the remarkable variation of EC and TDS. The average values of EC and TDS are significantly higher in thermal springs (EC=2532 µS/cm and TDS=1254 mg/L) than in cold waters (dug well EC=919 µS/cm and TDS=453 mg/L; tube well EC=1406 µS/cm and TDS=695 mg/L; natural spring EC=352 µS/cm and TDS=167 mg/L; stream EC=1838 µS/cm and TDS=906 mg/L). Both thermal springs and cold water have neutral conditions in nature (pH from 6.7 to 7.7). The average oxidation-reduction potential (ORP) indicates a slightly anoxic condition for thermal water (–32 mV) and oxidized condition for cold water (Range 0–16 mV). The maximum wellhead temperature of the thermal springs is 47 to 55 °C in Mahaoya springs, whereas the wellhead temperature of non-thermal water ranged from 27 to 32 °C.

#### 4.3. Classification of thermal water and cold water

Classification based on major cations and anions can act as a track record for water-rock interaction (Aksoy et al., 2009; Navarro et al., 2011; Baioumy et al., 2015). Major ions in Mahaoya and Marangala water implied that processes governing mineralization are occurring (Dissanayake and Munasinghe, 1984; Kröner et al.,

**Table 1**  
Statistical summary of cations and anions in thermal water and cold water.

	Thermal spring (n = 10)				Dug well (n = 112)				Tube well (n = 10)			
	AVG	MIN	MAX	SD	AVG	MIN	MAX	SD	AVG	MIN	MAX	SD
pH	7.7	7.1	8.0	0.3	7.0	6.2	7.6	0.3	6.8	6.8	6.9	0.1
ORP (mV)	−32	−44	−9	20	0.5	−42	46	21	11	10	11	1
EC ( $\mu\text{S}/\text{cm}$ )	2532	837	6460	2579	919	267	8730	1113	1406	830	2850	983
TDS (mg/L)	1254	410	3221	1285	453	128	4351	555	695	407	1415	492
Cation (mg/L)												
Li	0.25	0.15	0.53	0.16	0.14	0.01	0.46	0.18	0.15	0.04	0.44	0.18
Na	427	198	535	148	93	6	649	138	145	28	480	162
K	18	14	33	5	6	1	106	11	11	3	32	10
Ca	59	17	88	29	35	1	109	28	42	3	110	46
Mg	0.85	0.62	1.25	0.27	3.16	0.10	40.09	5.18	4.19	0.30	22.77	8.37
Rb	0.06	0.03	0.12	0.04	0.01	0.01	0.06	0.01	0.02	0.06	0.12	0.05
Sr	0.96	0.73	1.56	0.35	0.41	0.03	1.80	0.44	0.64	0.14	1.63	0.56
Cu	0.01	0.01	0.04	0.02	0.02	0.001	0.19	0.03	0.02	0.01	0.05	0.02
Zn	0.01	0.001	0.04	0.02	0.03	0.001	0.47	0.06	0.05	0.001	0.12	0.04
Pb	ND	ND	ND	ND	ND	ND	ND	ND	ND	ND	ND	ND
Mn	0.09	0.01	0.27	0.08	0.12	0.01	2.33	0.32	0.27	0.01	1.41	0.51
Fe	0.01	0.001	0.02	0.01	0.80	0.001	13.82	1.50	0.43	0.001	1.12	0.38
Al	2.50	2.29	2.67	0.14	2.03	0.01	28.43	6.10	3.95	2.10	5.43	1.69
Ba	0.97	0.72	1.22	0.21	1.84	0.06	3.56	1.17	2.43	1.61	3.28	0.75
Be	0.34	0.28	0.45	0.06	0.07	0.01	0.38	0.10	0.16	0.01	0.36	0.17
Anion (mg/L)												
F	6.9	2.2	14.0	6.4	3.6	0.1	15.9	4.5	8	0.5	15	8
SO	280	201	467	117	41	2	591	71	55	12	179	65
CO/HC	101	25	195	64	250	49	1325	210	406	171	725	234
Cl	88	26	120	41	42	2	280	37	136	28	415	143
Natural spring (n = 5)												
	AVG	MIN	MAX	SD	River/stream (n = 5)							
					AVG	MIN	MAX	SD				
pH	6.7	6.5	7.0	0.2	7.0	6.6	7.5	0.6				
ORP (mV)	16	2	30	14	9	−34	27	36				
EC ( $\mu\text{S}/\text{cm}$ )	352	200	482	142	1838	1715	1960	173				
TDS (mg/L)	167	93	233	70	906	844	967	87				
Cation (mg/L)												
Li	0.43	0.42	0.45	0.02	0.43	0.41	0.44	0.02				
Na	8.80	7.74	9.92	1.09	39.67	25.88	53.45	19.49				
K	1.21	0.48	1.78	0.66	3.96	3.56	4.36	0.56				
Ca	1.86	1.29	2.75	0.78	12.21	8.63	15.80	5.07				
Mg	3.04	1.27	3.99	1.53	8.12	3.07	13.17	7.14				
Rb	0.04	0.03	0.04	0.01	0.04	0.03	0.05	0.01				
Sr	0.94	0.90	0.98	0.04	1.14	1.05	1.23	0.13				
Cu	0.03	0.01	0.05	0.02	0.03	0.01	0.05	0.03				
Zn	0.01	0.001	0.03	0.02	0.01	0.001	0.02	0.01				
Pb	ND	ND	ND	ND	ND	ND	ND	ND				
Mn	0.05	0.02	0.09	0.04	0.06	0.02	0.10	0.05				
Fe	0.14	0.03	0.20	0.09	0.35	0.01	0.69	0.48				
Al	ND	ND	ND	ND	ND	ND	ND	ND				
Ba	ND	ND	ND	ND	ND	ND	ND	ND				
Be	ND	ND	ND	ND	ND	ND	ND	ND				
Anion (mg/L)												
F	0.05	0.02	0.08	0.04	1.19	0.83	1.54	0.50				
SO	21	16	27	6	85	27	144	83				
CO/HC	89	49	122	37	183	122	244	86				
Cl	3	2	4	1	12	6	18	8				

1991), and this can be generally observed around a geothermal field (Navarro et al., 2011).

The thermal and cold water from Mahaoya and Marangala were classified using a Piper plot (Fig. 2; Piper, 1953). The plot indicates that Na, K, and  $\text{SO}_4$  are the dominant ions in thermal water, whereas the cold water exhibits an unstable chemistry, as has been shown in other geothermal fields (Han et al., 2010). In contrast, the thermal waters are saline (Avg EC = 2532  $\mu\text{S}/\text{cm}$  and Avg TDS = 1254 mg/L) and characterized by a dominant Na-K- $\text{SO}_4$  composition, which may indicate deep circulations (Figs. 2 and 6). However, cold water contains a Na-K- $\text{HCO}_3$  type, which may be due to influence from deep groundwater by iron exchange, most likely between the thermal water and host geology (Piper, 1953). Shallow cold water and

surface springs typically have a Ca- $\text{HCO}_3$  type due to meteoric origin (Fig. 2). In contrast, streams demonstrate a Na-K- $\text{SO}_4$  composition due to accumulation of overflowed thermal water from the wells.

Ternary diagrams were used to help map the water type (Fig. 3; Baioumy et al., 2015). The diagrams further illustrate a K-Na- $\text{SO}_4$ -rich composition for the thermal water, as presented in the classification. Similar to Piper discrimination, the cold water samples are plotted in the  $\text{HCO}_3$ , Cl, and  $\text{SO}_4$  fields, which show Ca- $\text{HCO}_3$ -, Na-K- $\text{HCO}_3$ -, and Na-K- $\text{SO}_4$ -type waters (Fig. 3a). In addition, the thermal and cold water indicate trends from Na to  $\text{SO}_4$ , and from Na + K to Ca (Fig. 3b and c), which corresponds to

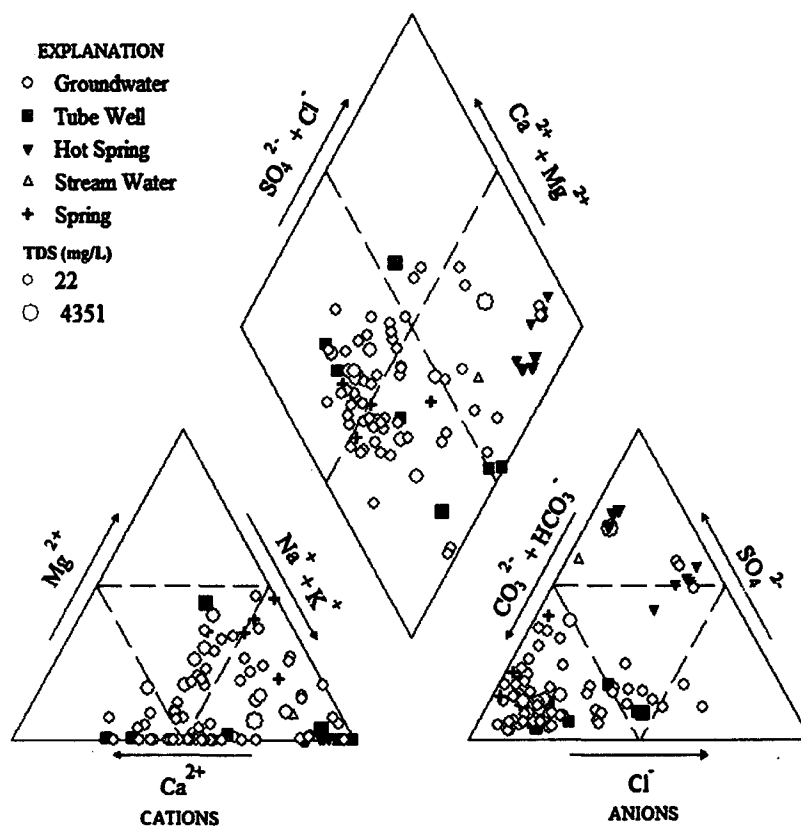


Fig. 2. Classification of thermal water and cold water using a Piper diagram (Piper, 1953).

the lower Mg content in the geothermal fields of Mahaoya and Marangala (Table 1).

#### 4.4. Chemical geothermometry of Mahaoya and Marangala

Geothermometers are based on temperature-dependent water-rock equilibria (Nicholson, 1993). Based on the chemical constituents of thermal water, several geothermometers were introduced to calculate reservoir temperature (Truesdell, 1976; Kharaka et al., 1982; Arnórsson et al., 1983; Giggenbach, 1988; Kharaka and Mariner, 1989). The reservoir temperatures calculated using cation geothermometry for Mahaoya and Marangala springs span a wide range (Table 2). The Na/K geothermometers from Arnórsson et al. (1983) yielded the highest temperature for both Mahaoya (148 °C) and Marangala (191 °C). Those values are slightly higher than those obtained using silica geothermometers, as shown in other non-volcanic thermal springs (Baïoumy et al., 2015).

The Na-K-Mg relationship is a combination of Na-K and K-Mg geothermometers (Giggenbach, 1988). It can recognize water types and evaluate aquifer temperature, which attained equilibrium with the host lithology (Pasvanoglu and Chandrasekharan, 2011). Mahaoya and Marangala samples from this study demarcate a wide range of temperature in the Na-K-Mg plot (Fig. 4a). This wide range of temperature is mainly governed by the rate of re-equilibration of Na, K, and Mg during water-rock interactions. Thus, the Na-K geothermometer shows high-temperature deep equilibria due to slow and intermediate re-equilibration rates of Na and K, respectively (Giggenbach, 1988; Han et al., 2010). As shown in Fig. 4a, geothermal springs of Mahaoya and Marangala yielded partially equilibrated and immature fields, and this most likely represents the extent of equilibration in the reservoir (Giggenbach, 1988). For instance, Marangala thermal springs produce higher tempera-

ture values for Na-K geothermometers (from 191 to 155 °C), which usually suggests deep water-rock equilibria. Calculated geothermometers of Na-K for Mahaoya springs indicate relatively lower reservoir temperature (from 101 to 148 °C), which implies more shallow equilibration than Marangala thermal springs. This suggests that the Marangala geothermal reservoir is located at a deeper level than the Mahaoya.

The K-Mg geothermometer is also a relationship, which due to a slightly faster equilibrium process than Na-K (Giggenbach, 1988). Because the Na-K geothermometer is sensitive to CO<sub>2</sub> pressure of a geothermal fluid, it has slower equilibrium. This indicates low-temperature intermediate depth equilibria due to intermediate and fast re-equilibration rate of K and Mg, respectively. Hence, Mahaoya and Marangala springs yielded equilibrium temperatures from the K-Mg geothermometer that are lower than those from the Na-K geothermometer; this implies an intermediate depth equilibration process. The reservoir temperatures of Mahaoya and Marangala were 120 °C and 105 °C, respectively.

In contrast, based on both Na-K and K-Mg geothermometers, the Na-K-Mg plot in Fig. 4 shows that the Mahaoya geothermal reservoir points to a process of deep to intermediate depth equilibration (148–101 °C). Marangala reservoir equilibration reveals a similar trend, but its reservoir depth appears to be much deeper than Mahaoya (176–105 °C).

The SiO<sub>2</sub>-quartz geothermometers often yield rather similar equilibrium temperatures to the K-Mg geothermometer (Fournier, 1977; Han et al., 2010). According to Chandrajith et al. (2013), the Mahaoya reservoir provides an intermediate equilibration based on silica-quartz and silica-chalcedony geothermometers (92–131 °C). The Marangala reservoir indicates very shallow equilibration (57–98 °C) with respect to the wellhead temperature (45 °C). However, based on the modified silica geothermometer, both Mahaoya and Marangala show intermediate equilibration (Table 2; Verma and Santoyo, 1997).

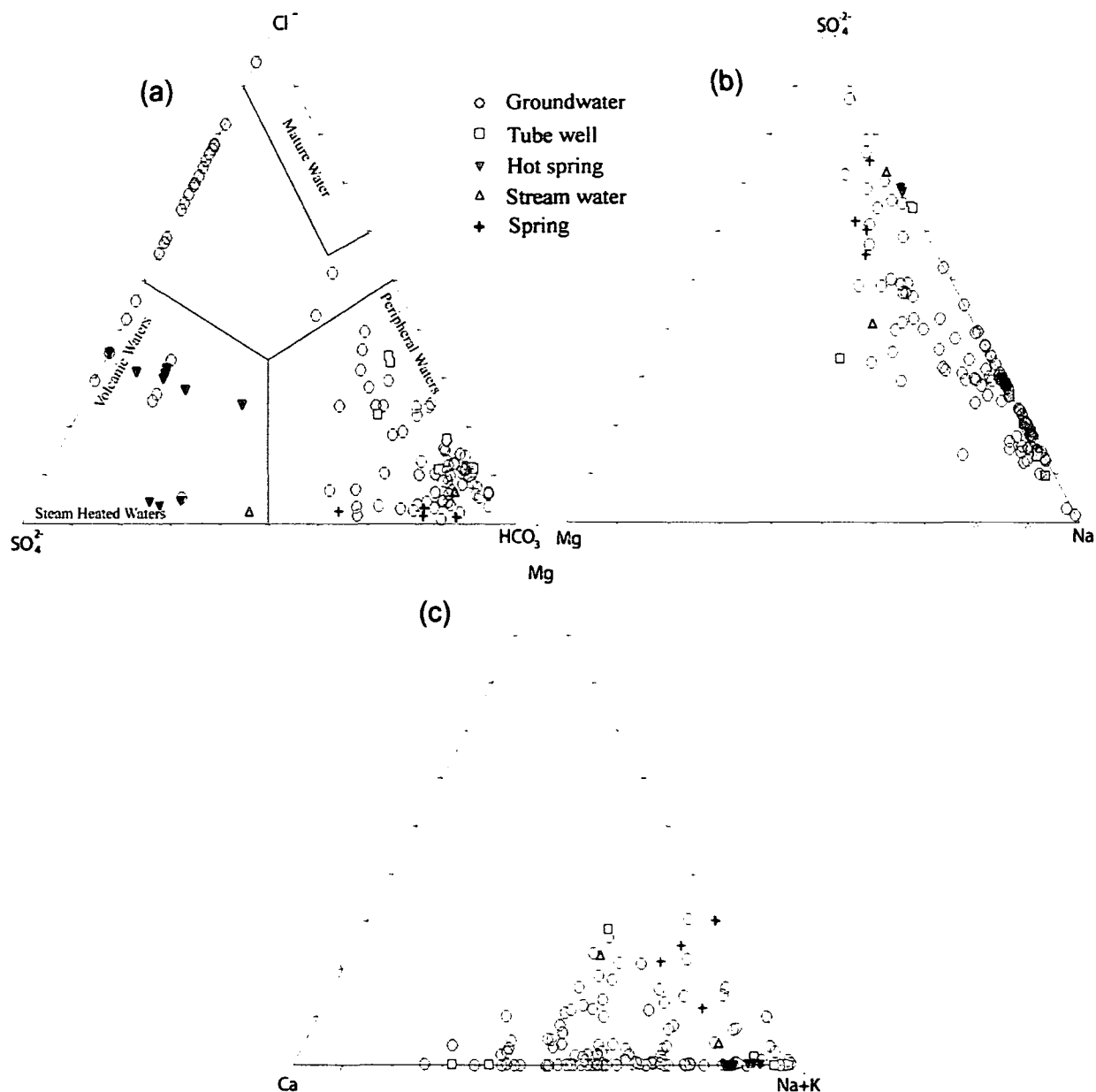


Fig. 3. Classification of water using triangular plots for major cations and anions (after Baioumy et al., 2015).

The groundwater sample plot in the immature field indicates water-rock interactions during flow or mixing with cold groundwater have not reached ionic equilibrium. Furthermore, many cold water samples are fully equilibrated, which may suggest lack of water-rock interactions. The  $10\text{Mg}/(10\text{Mg} + \text{Ca})$  versus  $10\text{K}/(10\text{K} + \text{Na})$  express similar behavior with the Na-K-Mg relationship. Thus, the thermal waters and some groundwater from Mahaoya and Marangala attain a full equilibrium line in the  $10\text{Mg}/(10\text{Mg} + \text{Ca})$ - $10\text{K}/(10\text{K} + \text{Na})$  binary plot (Fig. 4b). Conversely, thermal waters and most cold water have not reached the equilibrium state.

#### 4.5. Possible water-rock interaction and element correlation

Water-rock interaction increases salinity of thermal water, and composition depends on basement mineralogy and reservoir temperature (Brantley et al., 2007). In particular, Na-K-Ca-Cl-S-bearing minerals can dissolve under higher temperature of a geotherm (Greenberg and Møller, 1989; Freyer and Voigt, 2004). In con-

trast, Mahaoya and Marangala geothermal waters are considered to be saturated by quartz and chalcedony (Chandrajith et al., 2013), whereas our study denotes saturation from feldspar, mica, and amphibole in the basement.

The concentration of selected ions and ionic ratios were plotted against Cl and presented in Fig. 5. Element correlations of Cl with Na ( $R^2 = 0.60$ ;  $p < 0.01$ ) and K ( $R^2 = 0.65$ ;  $p < 0.01$ ) indicate decreasing dilution trends from thermal springs to cold water (Fig. 5a and b). The relationship between those elements may indicate the water-rock interaction of thermal water with minerals such as alkali feldspar, apatite, biotite, muscovite, and amphibole in the basement rocks (Fig. 1; Cooray, 1994; Teiber et al., 2014). Those minerals are unstable under high temperature; hence, labile Na, K, and Cl of mineral phases dissolve in thermal water (Halder and Tišljarić, 2014). Conversely, lower values of Na, K, and Cl in cold water may reflect the stability of those minerals under low temperature conditions.

The scatter distribution of Ca/Cl versus Cl ( $R^2 = 0.27$ ;  $p < 0.01$ ) represents variable concentrations of Ca and Cl in the water;

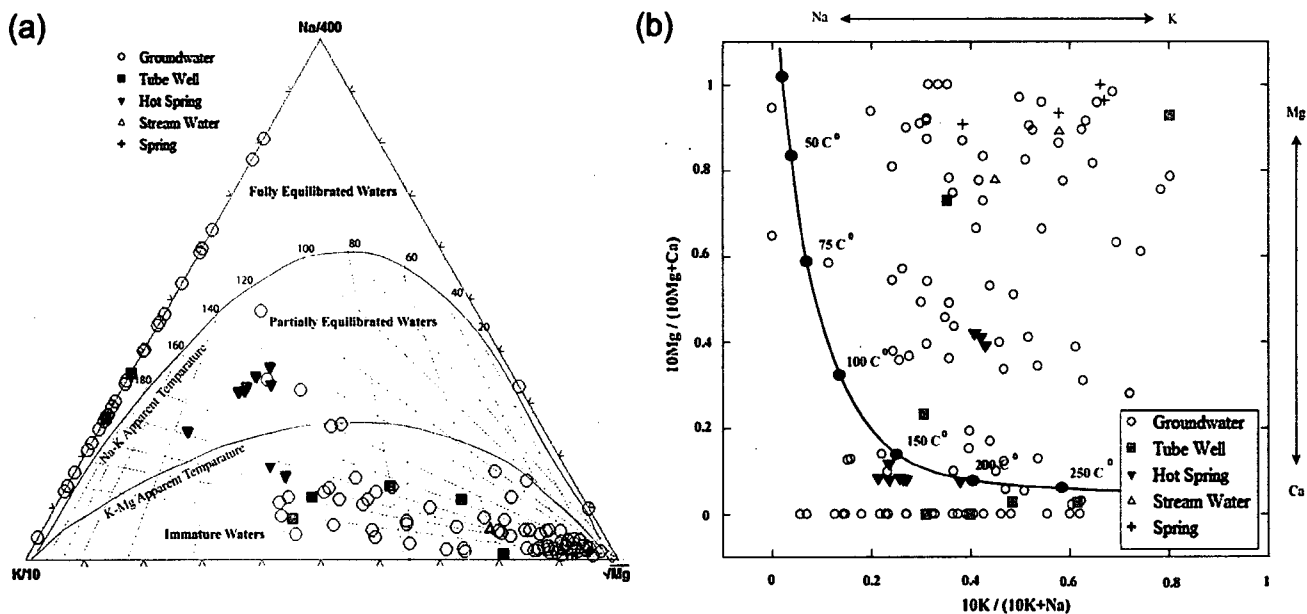


Fig. 4. Assessment of subsurface temperatures and water-rock equilibrium using (a) Na-K-Mg diagram of Giggenbach (1988) and (b) binary 10Mg/(10Mg+Ca) vs. 10K/(10K+Na) diagram.

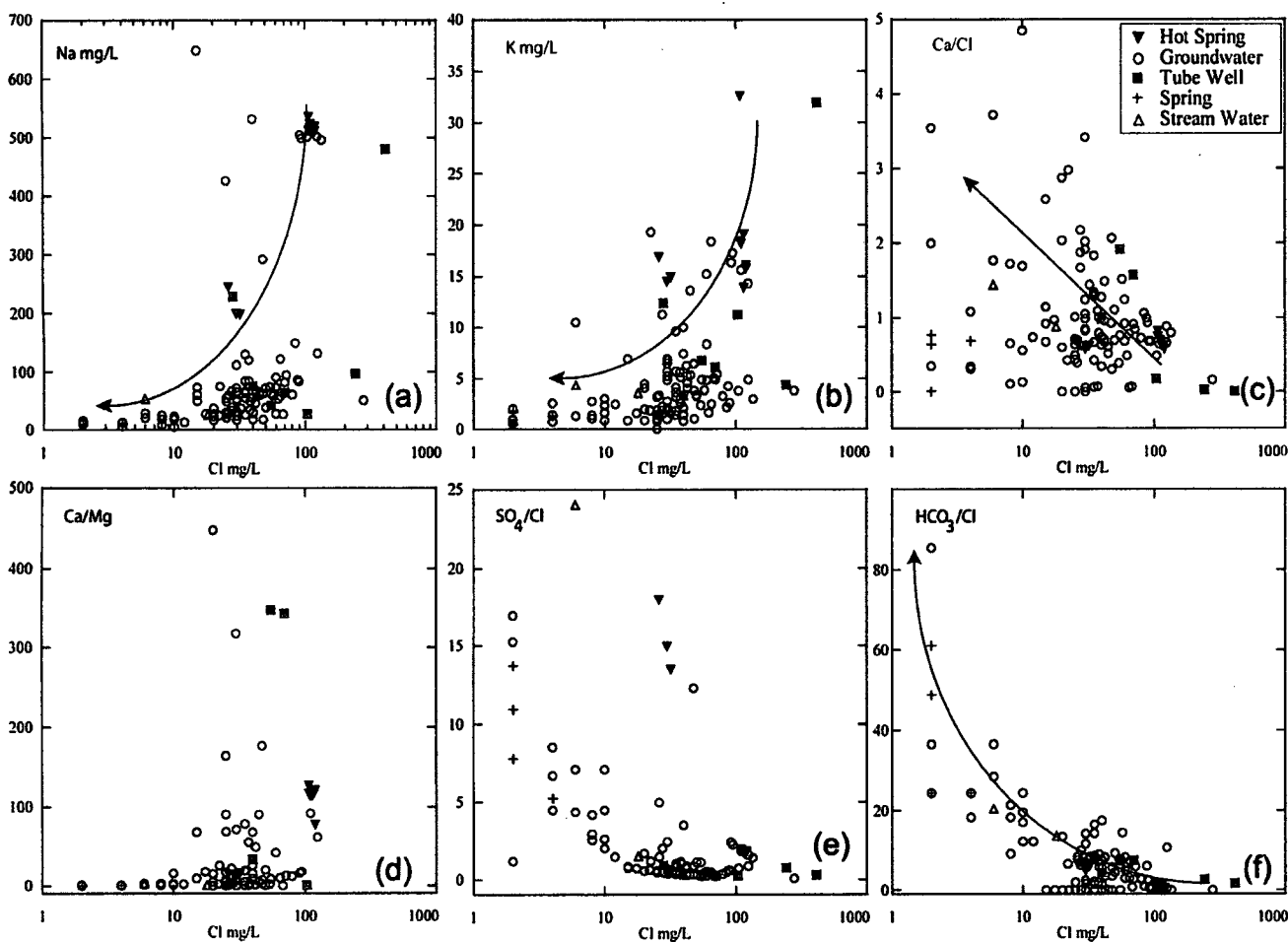


Fig. 5. Plots of ions and ion ratios versus chloride concentration for different water samples in Mahaoya and Marangala non-volcanic geothermal fields.

Please cite this article in press as: Jayawardana, D.T., et al., Mixing geochemistry of cold water around non-volcanic thermal springs in high-grade metamorphic terrain, Sri Lanka. *Chemie Erde - Geochemistry* (2016), <http://dx.doi.org/10.1016/j.chemer.2016.10.003>



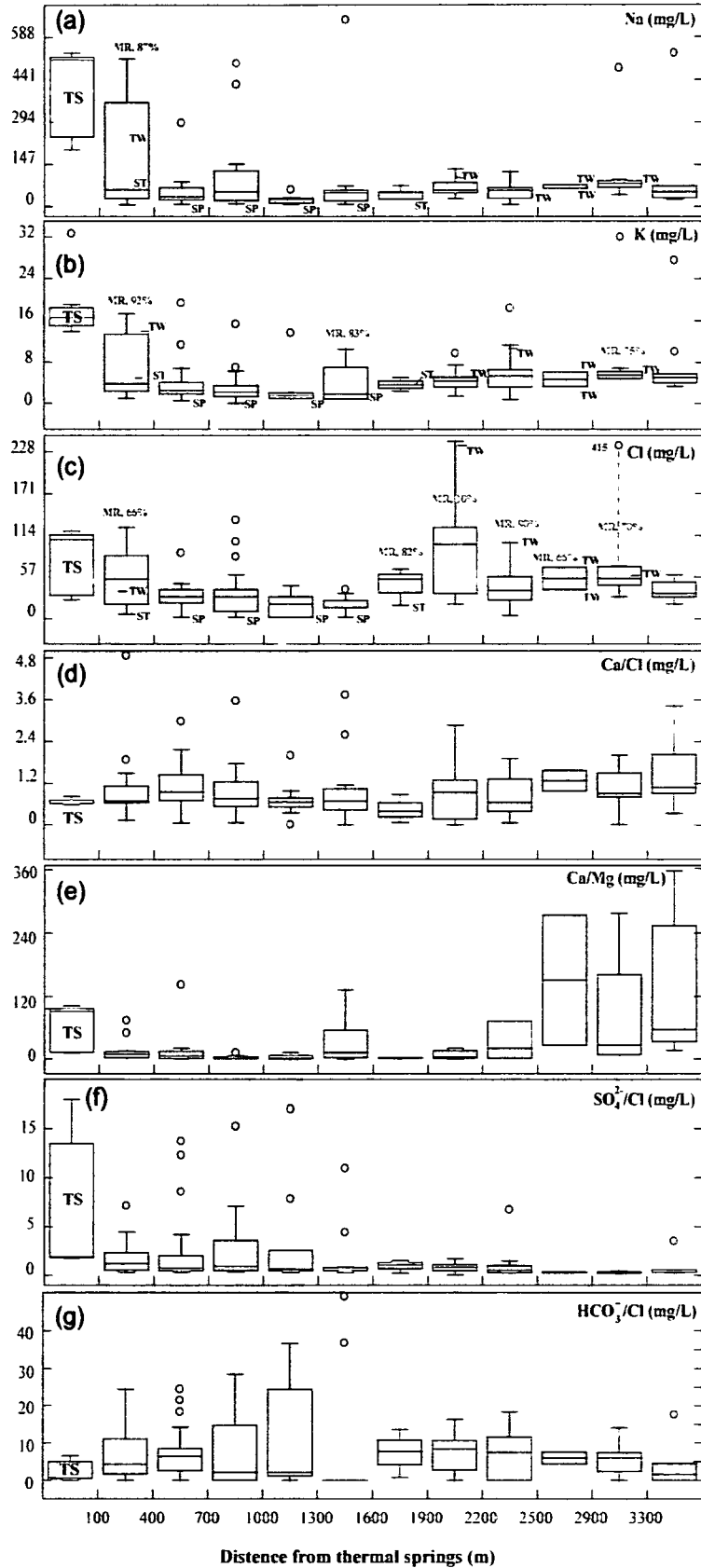


Fig. 6. Box and whisker plots for ions and ion ratios with respect to distance from thermal springs [The boxes show the mean value and quartiles; the smallest and largest values are indicated by the small horizontal line at the end of the whisker; and open circle denote outliers], TS thermal spring, TW tube well, ST stream, SP spring, and MR mixing ratio.

Please cite this article in press as: Jayawardana, D.T., et al., Mixing geochemistry of cold water around non-volcanic thermal springs in high-grade metamorphic terrain, Sri Lanka. *Chemie Erde - Geochemistry* (2016), <http://dx.doi.org/10.1016/j.chemer.2016.10.003>

Table 2

Geothermometric calculations of reservoir temperatures using cation geothermometers for non-volcanic thermal fields in Mahaoya and Marangala, Sri Lanka.

	Mahaoya (T °C)	Marangala (T °C)
Cation geothermometers (This study)		
Na/K (Arnósson et al., 1983) <sup>a</sup>	121	176
Na/K (Arnósson et al., 1983) <sup>b</sup>	148	191
Na/K, (Truesdell, 1976) <sup>c</sup>	101	155
K/Mg (Giggenbach, 1988) <sup>d</sup>	120	105
Na/Li (Kharaka et al., 1982) <sup>e</sup>	96	189
Li/Mg (Kharaka and Mariner, 1989) <sup>f</sup>	81	103
Silica geothermometers (Chandrajith et al., 2013)		
Silica–quartz conductive cooling	131	97
Silica quartz max. steam loss	128	98
Silica–Chalcedony	92	57
Silica–Chalcedony	103	68
Modified silica geothermometer	121	138

Equations for cation geothermometers:

<sup>a</sup>  $t = 933 / (0.933 + \log \text{Na/K}) - 273.15$ .

<sup>b</sup>  $t = 1319 / (1.699 + \log \text{Na/K}) - 273.15$ .

<sup>c</sup>  $t = 856 / (0.857 + \log \text{Na/K}) - 273.15$ .

<sup>d</sup>  $t = 4410 / (13.95 + \log \text{K}^2/\text{Mg}) - 273.15$ .

<sup>e</sup>  $t = 1590 / (0.779 + \log (\text{Na/Li})) - 273.15$ .

<sup>f</sup>  $t = 2200 / (5.470 - \log (\text{Li/Mg}^{0.5})) - 273.15$ .

higher ratios of Ca/Cl in cold water are common for Mahaoya and Marangala (Fig. 5c). Weathering of plagioclase feldspar bearing granitic rocks, and calcite- and dolomite-bearing marble are the probable sources for Ca in water (Fig. 1; Cooray, 1994). Those minerals are unstable at low temperatures; thus, Ca is effectively released in cold water (Haldar and Tišljarić, 2014). Therefore, higher values of Ca represent the dug wells (Range, 35–109 mg/L) and tube wells (Range, 42–110 mg/L) rather than the thermal water (Range, 59–88 mg/L).

Mahaoya and Marangala water samples are characterized by lower concentrations of Mg, Fe, Pb, Zn, and Cu, which demonstrate lack of ferromagnesian minerals in the bedrock (Table 1; Nesbitt and Young, 1996; Sharma and Rajamani, 2001). Thus, the higher Ca/Mg ratio of some samples in Ca/Mg vs. Cl ( $R^2 = 0.29$ ;  $p < 0.01$ ) plot is due to depletion of Mg and enrichment of Ca in thermal and cold water (Fig. 5d).

The  $\text{SO}_4$  usually indicates deep water-rock equilibria in the geothermal system. Relatively higher  $\text{SO}_4/\text{Cl}$  ratios in Marangala springs are distinct (Fig. 5e), which may represent more deeply originated water than in Mahaoya springs. However, most of the cold water provides lower  $\text{SO}_4/\text{Cl}$  ratios under improved physical conditions in the wells (Table 1). Thermal springs and most cold waters indicate lower  $\text{HCO}_3/\text{Cl}$  ratios (Fig. 5f), which suggests thermal water flows through a long subsurface flow path and deep water. Higher  $\text{HCO}_3/\text{Cl}$  ratios in cold water indicate a shorter flow path and faster water cycle.

#### 4.6. Lateral mixing of cold water

Mixing of thermal water with cold water is specific to a geothermal field, and it has been widely investigated (Gemici and Tarcan, 2002; Serpen, 2004; Aksoy et al., 2009; Navarro et al., 2011; Taran et al., 2013; Petrini et al., 2013). Mixing dilutes the geothermal water and declines the temperature of the reservoir (Gibson and Hinman, 2013). The lateral mixing of Mahaoya and Marangala geothermal systems in Sri Lanka appears to be controlled by structures in the bedrock (Fig. 1) because groundwater flow is effectively controlled by deep fractures and faults in the trust zone (Panabokke and Perera, 2005; Dissanayake and Munasinghe, 1984).

Evaluation of mixing using box and whisker plots for selected elements is illustrated in Fig. 6. Due to identical geology and hydrogeology, Mahaoya and Marangala geochemical data are considered together in the plots (Fig. 1). The figure reveals a clear contrast of mixing with increasing distance from the thermal springs. In con-

trast, Na, K, and Cl concentrations are high in the nearest cold water wells (<400 m) due to mixing from ascending of thermal water (Fig. 6a–c; Fig. 7; Gibson and Hinman, 2013). Concentrations of Na and K significantly declines in cold water after 400 m due to isolation of rain fed water. However, abnormal Na, K, and Cl values (outliers in Fig. 6a–c; Fig. 7) are reported in some deep wells located away from the thermal springs, and indicate different levels of mixing ratios. This may suggest deeply circulated geothermal water along the shear zones (Fig. 7; Han et al., 2010; Gibson and Hinman, 2013).

Element ratios also reflect different geochemical behaviors in Mahaoya and Marangala. Thermal water shows the lowest value of Ca/Cl, and the highest ratios are recorded from the most distant cold water wells (Fig. 6d; Fig. 7). The ratio of Ca/Mg indicates a similar trend for distant cold water, whereas thermal water shows a moderate level of Ca/Mg (Fig. 6e). The relationships of Ca/Cl and Ca/Mg may imply a lack of Mg-bearing minerals for water-rock interaction around the geothermal field. The ratio for  $\text{SO}_4/\text{Cl}$  seems to gradually decline with increasing distance from thermal water, which may be due to oxidation of  $\text{SO}_4$  to  $\text{H}_2\text{S}$  when moving away from the thermal springs. However, some abnormal levels of  $\text{SO}_4/\text{Cl}$  (outliers in Fig. 6f) in near cold water wells may indicate deep circulations (Kumara and Dharmagunawardhane, 2014). Variable extent of  $\text{HCO}_3/\text{Cl}$  clearly indicates different impacts of meteoric water on sub-surface thermal water flow (Fig. 6g; Fig. 7).

## 5. Conclusions

The non-volcanic thermal reservoir in metamorphic terrain extends from intermediate to deeper depths. This indicates higher reservoir temperatures for Na-K-Mg, Na-Li, and Li-Mg geothermometry. It is also evident that those reservoirs are potential sources of geothermal energy. Hydrogeochemistry of thermal waters is distinct from that of cold water; the higher contents of some cations and anions in the thermal water are most likely due to water-rock interaction with feldspar, mica, and sulfide minerals in the granitic basement. Conversely, lower values of ferromagnesian minerals in the basement were observed. It is concluded that classification of thermal water and cold water for both Mahaoya and Marangala is due to iron exchange in the deep groundwater and deep circulations of thermal water through the fractures and faults. Therefore, a clear contrast is evident as thermal water and cold water are mixed with increasing distance from the geothermal fields.

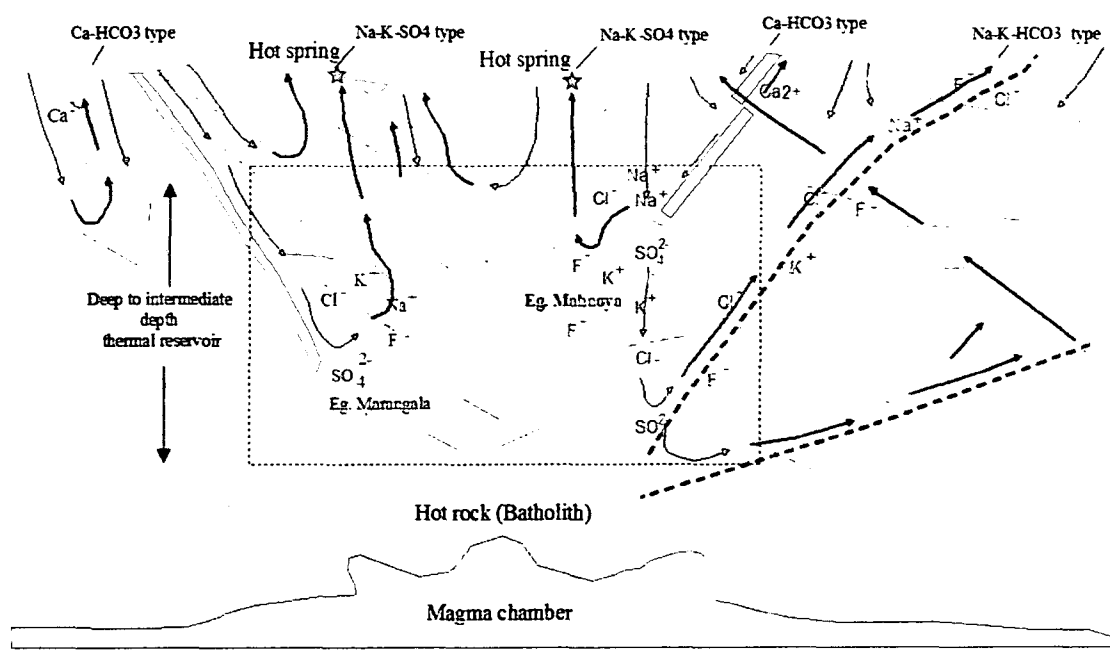


Fig. 7. Schematic diagram of the Mahaoya and Marangala geothermal system illustrating possible water-rock interaction and mixing. Dotted line rectangle denotes possible geothermal reservoir. Groundwater movement is indicated by arrows; thinner lines represent fractures; and heavy dashed lines are shear zones. Legend for the conceptual rock layers is provided in Fig. 1.

**Acknowledgments**

We wish to thank the dean of the Faculty of Science and Technology, Uva Wellassa University, Sri Lanka, for the support provided during the field and laboratory research. We extend our gratitude to the University Research Council, Sri Jaywardenepura University, Sri Lanka, for granting support.

**References**

Ahmed, F., Bibi, M.H., Ishiga, H., Fukushima, T., Maruoka, T., 2010. Geochemical study of arsenic and other trace elements in groundwater and sediments of the Old Brahmaputra River Plain, Bangladesh. *Environ. Earth Sci.* 60, 1303–1316.

Aksoy, N., Simsek, C., Gunduz, O., 2009. Groundwater contamination mechanism in a geothermal field: a case study of Balçova, Turkey. *J. Contam. Hydrol.* 103, 13–28.

Arnórsón, S., Gunnlaugsson, E., Svavarsón, H., 1983. The chemistry of geothermal waters in Iceland: III. *Chem. Geother. Geotherm. Investig. Geochim. Cosmochim. Acta* 47, 567–577.

Baioumy, H., Nawawi, M., Wagner, K., Arifin, M.H., 2015. Geochemistry and geothermometry of non-volcanic hot springs in West Malaysia. *J. Volcanol. Geotherm. Res.* 290, 12–22.

Brantley, S., Kubicki, J., White, A., 2007. *Kinetics of water-rock interaction*. Springer, New York USA, pp. pp 73–102.

Brugger, J., Long, N., McPhail, D.C., Plimer, I., 2005. An active amagmatic hydrothermal system: the Paralana hot springs, Northern Flinders Ranges, South Australia. *Chem. Geol.* 222, 35–64.

Capasso, G., Alessandro, W.D., Favara, R., Inguaggiato, S., Parello, F., 2001. Interaction between the deep fluids and the shallow groundwaters on Vulcano island (Italy). *J. Volcanol. Geotherm. Res.* 108, 187–198.

Chandrajith, R., Barth, J.A.C., Subasinghe, N.D., Merten, D., Dissanayake, C.B., 2013. Geochemical and isotope characterization of geothermal spring waters in Sri Lanka: evidence for steeper than expected geothermal gradients. *J. Hydrol.* 476, 360–369.

Chandrapala, L., Wimalasuriya, M., 2003. Satellite measurements supplemented with meteorological data to operationally estimate evaporation in Sri Lanka. *Agric. Water Manage.* 58, 89–107.

Chandrasekharam, D., Antu, M.C., 1995. *Geochemistry of Tattapani thermal springs, Madhya Pradesh, India—field and experimental investigations*. *Geothermics* 24, 553–559.

Cooray, P.G., 1984. An introduction to the geology of Sri Lanka (Ceylon), 2nd revised edition. National museum publication, Colombo, pp. 81–104, 256–259, 289.

Cooray, P.G., 1994. The precambrian of Sri Lanka: a historical review. *Precambrian Res.* 66, 3–18.

Dissanayake, C.B., Jayasena, H.A.H., 1988. Origin of geothermal systems of Sri Lanka. *Geothermics* 17, 657–669.

Dissanayake, C.B., Munasinghe, T., 1984. Reconstruction of the Precambrian sedimentary basin in the granulite belt of Sri Lanka. *Chem. Geol.* 47, 221–247.

Dissanayake, C.B., Weerasooriya, S.V.R., 1986. Fluorine as an indicator of mineralization hydrogeochemistry of a Precambrian mineralized belt in Sri Lanka. *Chem. Geol.* 56, 257–270.

Du, J., Liu, C., Fu, B., Ninomiya, Y., Zhang, Y., Wang, C., Wang, H., Sun, Z., 2005. Variations of geothermometry and chemical-isotopic compositions of hot spring fluids in the Rehai geothermal field, southwestern China. *J. Volcanol. Geotherm. Res.* 142, 243–261.

Ensaifi, A.A., Kazemzadeh, A., 1999. Simultaneous determination of nitrite and nitrate in various samples using flow injection with spectrophotometric detection. *Anal. Chim. Acta* 382, 15–22.

Favara, R.O., Grassa, F., Inguaggiato, S., Valenza, M., 2001. Hydrogeochemistry and stable isotopes of thermal springs: earthquake-related chemical changes along Belice Fault (Western Sicily). *Appl. Geochem.* 16, 1–17.

Fournier, R.O., 1977. Chemical geothermometers and mixing models for geothermal systems. *Geothermics* 5, 41–50.

Freyer, D., Voigt, W., 2004. The measurement of sulfate mineral solubilities in the Na-K-Ca-Cl-SO<sub>4</sub>-H<sub>2</sub>O system at temperatures of 100, 150 and 200 °C. *Geochim. Cosmochim. Acta* 68, 307–318.

Gemici, U., Tarcan, G., 2002. *Hydrogeochemistry of the Simav geothermal field, Western Anatolia, Turkey*. *J. Volcanol. Geotherm. Res.* 116, 215–233.

Gibson, M.L., Hinman, N.W., 2013. Mixing of hydrothermal water and groundwater near hot springs, Yellowstone National Park (USA): hydrology and geochemistry. *Hydrol. J.* 21, 919–933.

Giggenbach, W.F., 1988. Geothermal solute equilibria: derivation of Na-K-Mg-Ca geothermometers. *Geochim. Cosmochim. Acta* 52, 2749–2765.

Greenberg, J.P., Møller, N., 1989. The prediction of mineral solubilities in natural waters: a chemical equilibrium model for the Na-K-Ca-Cl-SO<sub>4</sub>-H<sub>2</sub>O system to high concentration from 0 to 250 °C. *Geochim. Cosmochim. Acta* 53, 2503–2518.

Haldar, S.K., Tišljarić, J., 2014. *Introduction to mineralogy and petrology*. Chapter 4. In: *Igneous Rocks*. Elsevier Publication, pp. 93–120.

Han, D.M., Liang, X., Jin, M.G., Currell, M.J., Song, X.F., Liu, C.M., 2010. Evaluation of groundwater hydrochemical characteristics and mixing behavior in the Daying and Qicun geothermal systems, Xinzhou Basin. *J. Volcanol. Geotherm. Res.* 189, 92–104.

Herath, J.W., 1984. Geology and occurrence of gems in Sri Lanka. *J. Natl. Sci. Council Sri Lanka* 12, 257–271.

Jessop, A.M., Ghomshei, M.M., Drury, J.M., 1991. Geothermal energy in Canada. *Geothermics* 20, 369–385.

Kharaka, Y.K., Mariner, R.H., 1989. Chemical geothermometers and their application to formation waters from sedimentary basins. In: Näser, N.D., McCulloh, T.H. (Eds.), *Thermal History of Sedimentary Basins Methods and Case Histories*. Springer, Verlag, pp. 99–117.

Kharaka, Y.K., Lico, M.S., Law, L.M., 1982. Chemical geothermometers applied to formation waters, Gulf of Mexico and California Basins. *Am. Assoc. Pet. Geol. Bull.* 66, 558.

Kröner, A., Cooray, P.G., Vitanage, P.W., 1991. Lithotectonic subdivision of the Precambrian basement in Sri Lanka. In: Kröner, A. (Ed.), *The Crystalline Crust of*

Please cite this article in press as: Jayawardana, D.T., et al., *Mixing geochemistry of cold water around non-volcanic thermal springs in high-grade metamorphic terrain, Sri Lanka*. *Chemie Erde - Geochemistry* (2016), <http://dx.doi.org/10.1016/j.chemer.2016.10.003>

- Sri Lanka, Summary of Research of the German-Sri Lankan Consortium. Geological Survey Department, Sri Lanka, pp. 1–5.
- Kumara, S.M.P.G.S., Dharmagunawardhane, H.A., 2014. A geostructural model for the nelumwewa thermal spring: north central province, Sri Lanka. *J. Geol. Soc. Sri Lanka* 16, 19–27.
- Mangala, P.S., Wijetilake, S., 2011. The potential of geothermal energy resources in Sri Lanka. Geothermal training programme, Orkustofnun, Grensasvegur, Reykjavik, Iceland.
- Mutlu, H., Gulec, N., 1998. Hydrogeochemical outline of thermal waters and geothermometry, applications in Anatolia (Turkey). *J. Volcanol. Geotherm. Res.* 85, 495–515.
- Navarro, A., Fonta, X., Viladevall, M., 2011. Geochemistry and groundwater contamination in the La Selva geothermal system (Girona, Northeast Spain). *Geothermics* (in press).
- Nesbitt, H.W., Young, G.M., 1996. Petrogenesis of sediments in the absence of chemical weathering: effects of abrasion and sorting on bulk composition and mineralogy. *Sedimentology* 43, 341–358.
- Nicholson, K., 1993. *Geothermal Fluids: Chemistry and Exploration Techniques*. Springer-Verlag, Berlin, Heidelberg, p. 262.
- Nimalsiri, T.B., Suriyaarachchi, N.B., Hobbs, B., Manzella, A., Fonseka, M., Dharmagunawardana, H.A., Subasinghe, N.D., 2015. Structure of a low-enthalpy geothermal system inferred from magnetotellurics—a case study from Sri Lanka. *J. Appl. Geophys.* (in press).
- Panabokke, C.R., Perera, A.P.G.R.L., 2005. Groundwater Resources of Sri Lanka, Water Resources Board Sri Lanka, Special Report, pp. 3–13.
- Panabokke, C.R., 1996. Soils and agro-ecological environments of Sri Lanka. *Colombo Nat. Resour. Ser.*, 220.
- Papp, D.C., Nitoi, E., 2006. Isotopic composition and origin of mineral and geothermal waters from Tuşnad Băi Spa, Harghita Mountains, Romania. *J. Geochem. Explor.* 89, 314–317.
- Pasvanoğlu, S., Chandrasekharan, D., 2011. Hydrogeochemical and isotopic study of thermal and mineralized waters from the Nevşehir (Kozakli) area, Central Turkey. *J. Volcanol. Geotherm. Res.* 202, 241–250.
- Petrini, R., Italiano, F., Ponton, M., Slejko, F.F., Aviani, U., Zini, L., 2013. Geochemistry and isotope geochemistry of the Monfalcone thermal waters (northern Italy): inference on the deep geothermal reservoir. *Hydrol. J.* 21, 1275–1287.
- Piper, A.M., 1953. A graphic procedure in the geochemical interpretation of water analysis. USGS groundwater note no, Washington D.C. 12.
- Sanada, T., Takamatsu, N., Yoshiike, Y., 2006. Geochemical interpretation of long-term variations in rare earth element concentrations in acidic hot spring waters from Tamagawa geothermal area, Japan. *Geothermics* 35, 141–155.
- Senaratne, A., Chandima, D., 2011. Exploration of a potential geothermal resource at Wahawa Padiyatalwa area Sri Lanka. In: *Proceedings, Thirty-sixth Workshop on Geothermal Reservoir Engineering*, Stanford University, Stanford, California.
- Serpen, U., 2004. Hydrogeological investigations on Balçova geothermal system in Turkey. *Geothermics* 33, 309–335.
- Sharma, A., Rajamani, V., 2001. Weathering of charnockites and sediment production in the catchment area of the Cauvery River, southern India. *Chem. Geol.* 143, 169–184.
- Taran, Y., Morán-Zenteno, D., Inguaggiato, S., Varley, N., Luna-González, L., 2013. Geochemistry of thermal springs and geodynamics of the convergent Mexican Pacific margin. *Chem. Geol.* 339, 251–262.
- Teiber, H., Marks, M.A.W., Wenzel, T., Siebel, W., Altherr, R., Markl, G., 2014. The distribution of halogens (F, Cl, Br) in granitoid rocks. *Chem. Geol.* 274–275, 92–109.
- Truesdell, A.H., 1976. Summary of section III geochemical techniques in exploration. In: *Proceedings, Second United Nations Symposium on the Development and Use of Geothermal Resources*. San Francisco, 1975, Washington D.C., U.S. Government Printing Office.
- Verma, S.P., Santoyo, E., 1997. New improved equations for Na/K, Na/Li and SiO<sub>2</sub> geothermometers by outlier detection and rejection. *J. Volcanol. Geotherm. Res.* 79, 9–23.
- Villholth, K.G., Rajasooriyar, L.D., 2010. Groundwater resources and management challenges in Sri Lanka—an overview. *Water Resour. Manage.* 24, 1489–1513.
- Yaguchi, M., Muramatsu, Y., Chiba, H., Okumura, F., Ohba, T., Yamamuro, M., 2014. Hydrochemistry and isotopic characteristics of non-volcanic hot springs around the Miocene Kofu granitic complex surrounding the Kofu Basin in the South Fossa Magna region, central Honshu, Japan. *Geochem. J.* 48, 1–12.
- Zielinski, O., Voß, D., Saworski, B., Fiedler, B., Körtzinger, A., 2011. Computation of nitrate concentrations in turbid coastal waters using an *in situ* ultraviolet spectrophotometer. *J. Sea Res.* 65, 456–460.